ACS Sustainable Chemistry & Engineering

Research Article

pubs.acs.org/journal/ascecg

Hydrothermal Carbonization of Macroalgae and the Effects of Experimental Parameters on the Properties of Hydrochars

Qian Xu,[†] Qifeng Qian,[†] Augustine Quek,*[,†] Ning Ai,[‡] Ganning Zeng,[‡] and Jiawei Wang*[,†]

[†]Division of Engineering, University of Nottingham Ningbo China, 315100 Ningbo, China

[‡]College of Chemical Engineering and Materials Science, Zhejiang University of Technology, 310014, Hangzhou, China

ABSTRACT: Hydrochars derived from macroalgae *Sargassum horneri* were characterized physically and chemically to elucidate their potential as a valuable resource. Hydrochars were prepared by hydrothermal carbonization (HTC) of *Sargassum horneri* at temperatures of 180−210 °C with citric acid. The hydrochars were found to form mainly through a dehydration reaction pathway and had carbon contents of 36.8−50.5% and higher heating values of 19.0−25.1 MJ kg^{-1}. The BET surface area of hydrochars remained low, in the range of 0.6−31.8 m^2 g^{-1}. On the basis of Taguchi's experimental design, reaction temperature, reaction time, and particle size of feedstock were found to be the most important control factors for the chemical and physical properties of the hydrochars.

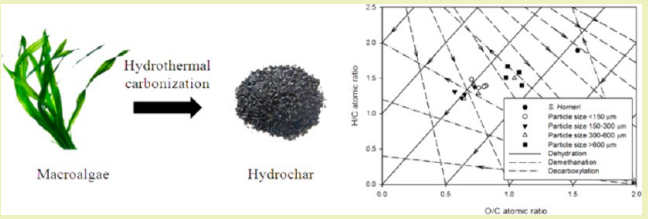

KEYWORDS: *Optimization, Macroalgae, Hydrothermal carbonization, Biomass, Sargassum horneri*

INTRODUCTION

Biomass is generally classified as a renewable resource, which can partially replace classical fossil fuel sources and enable reduction of carbon dioxide buildup in the atmosphere.[1] It can produce energy through direct burning or be converted into other types of fuel by various conversion technologies, such as pyrolysis, liquefaction, and gasification.[2] Among all these conversion technologies, hydrothermal carbonization (HTC) is a promising one. It converts biomass with low calorific value into a coal-like product, called hydrochar, under relative moderate conditions. The advantage of HTC is that biomass can be converted into carbonaceous solids without an energy-intensive drying process before or during the HTC process. It is especially important for feedstocks with high water content, like animal manures, sewage sludge, and marine biomass. More detailed discussions regarding HTC treatment of biomass can be found in recently published review articles by Titirici and Antonietti,[3] Hu et al.,[4] Libra et al.,[5] and Titirici et al.[6]

Compared to terrestrial biomass, marine biomass offers many advantages, including less demand on agricultural land and higher photosynthetic activity.[7] It has been successfully converted into methane, ethanol, and other biofuels through biological degradation or thermochemical treatments[8−11] and can also be used directly for combustion.[12,13] Although marine biomass has high potential for energy use, there are a few challenges in its applications, including high water content and high salt content. The HTC method has the potential to overcome some of the challenges, as it eliminates the need for a drying process before carbonization and is able to remove water-soluble salts during the process.

Recently, successful applications of the HTC method on marine biomass have been demonstrated on a few types of green and blue-green microalgae. Heilmann et al.[14] described char production from microalgae by relatively moderate conditions (190−210 °C). The produced hydrochar had a maximum heat of combustion of 31.58 MJ kg^{-1}, which is in the bituminous coal range. Carbon materials with high nitrogen content were also synthesized by the HTC method from *Spirulina platensis* in the temperature range of 180−240 °C.[15] The high nitrogen content in hydrochar was achieved because of the high protein fraction in microalgae. Unlike microalgae, no research on HTC on macroalgae has been reported so far.

Macroalgae, also called seaweeds, are multicellular macroscopic marine algae. They are also important contributors to marine biomass applications.[16] Compared to microalgae, which have high concentration of proteins, macroalgae possesses more plant-like characteristics. They comprise mainly cellulose, hemicellulose, and lignin. Therefore, macroalgae could be potential resources for hydrochar production like other lignocellulosic biomass.[17−20]

Sargassum horneri (*S. horneri*) (composition in Table 1) is one of the marine species that grows in the warmer temperate climates, being widely distributed along the warmer Chinese coastal areas. It can grow up to 3−5 m long and form underwater forests.[21] Because of its fast growth rate, *S. horneri* has been investigated for restoring marine ecosystems by providing small fishes a safe place to feed and spawn along the coast of Nanji

Table 1. *S. horneri* wt % Composition

cellulose	hemicellulose	lignin	other
37.9	21.8	19.7	20.6

Received: December 16, 2012
Revised: June 9, 2013
Published: June 18, 2013

Island, Wenzhuo City, China.[22] For mature *S. horneri* plants, it is important to find suitable applications as they are a form of waste, with decaying biomass producing unpleasant odors, depleting dissolved oxygen in shallow waters, and other environmental issues. Considering the advantages of the HTC method on marine biomass, mature *S. horneri* plants could be a good candidate to produce carbon materials.

The principal objective of the present work is to investigate the feasibility of using *S. horneri* as a feedstock for hydrochar production by the HTC method. The solid products were characterized using various analytical methods, including elemental analysis, thermogravimetric analysis (TGA), Fourier transform infrared (FTIR) spectroscopy, scanning electron microscopy (SEM), BET N_2 sorption, and bomb calorimeter. A secondary objective was to study the effects of operating parameters on the HTC process and the properties of produced hydrochars. Selected parameters included temperature, reaction time, amount of catalyst, and solid concentration. The Taguchi experimental method was applied to minimize the number of experiments required.

MATERIALS AND METHODS

Materials. Adult male and female *S. horneri* plants were sampled in April 2012 from the rocky shore at Nanji Islands, Wenzhou City, China. After sampling, the plants were air dried and delivered to the laboratory. For this study, the raw material was washed, ground, and sieved into four size classes: less than 150 μm, 150−300 μm, 300−600 μm, and greater than 600 μm. The powders were dried at 120 °C for 5 h, and then stored in a desiccator for further use. Citric acid monohydrate was purchased from Sinopharm (China) and used as received.

Hydrothermal Carbonization. The HTC process was carried out in a non-stirred 100 mL Teflon-lined stainless steel autoclave. A total of 10−80 mg of citric acid monohydrate was dissolved in 50 g distilled water in an autoclave. A total of 2.5−10 g of dried *S. horneri* powder was then added into the solution. The autoclave was sealed and transferred to a preheated oven. After being heated at 180−210 °C for 2−16 h, the autoclave was cooled to room temperature. The solid product was filtered, washed with distilled water, and finally dried at 120 °C for 5 h. The dried solid product was stored in a desiccator for further characterizations.

Characterizations. Elemental analysis (C, H, N, and S) of the samples was carried out on a PE 2400 Series II CHNS/O elemental analyzer. Oxygen content was determined by difference.

Proximate analysis was conducted using a thermogravimetric analyzer (Netzsch STA 449 F3). The temperature program was adapted from Munir et al.[23] The moisture content (MC) is determined by the mass loss after the sample is heated to 110 °C under N_2. The volatile matter (VM) corresponds to the mass loss between 110 and 910 °C under N_2. Fixed carbon (FC) is the solid combustible material that leads to the mass loss at 910 °C when the atmosphere is switched from N_2 to air. The residue left is ash content.

Scanning electron microscopic (SEM) images were recorded by a Hitachi S-4700 scanning electron microscope operating at 15 kV.

BET surface area and pore structure of the samples were determined by a Micromeritics ASAP 2420 using N_2 as the adsorbate at −195.85 °C. Prior to measuring, all of the samples were degassed at 150 °C for 16 h.

FT-IR spectra were collected in the range of 400−4000 cm^{-1} using a potassium bromide palletization method on a Nicolet iS10 FT-IR spectrometer. A total of 64 scans were taken for each interferogram at 4 cm^{-1} resolution.

The pH value of samples in water was determined according to Carrier et al.[24] A total of 0.5 g of sample was stirred with 10 mL distilled water for 60 min. The pH value of the suspension was measured after standing for 10 min with a pH meter (Denver Instrument).

The higher heating value (HHV) of samples was measured by an IKA C 200 Calorimeter system in the adiabatic mode.

Control Parameters and Taguchi Method. The conventional approach of experimenting with one variable at a time is time consuming and labor intensive. The Taguchi method provides an effective way to optimize experimental designs. A similar approach was used to investigate the hydrothermal carbonization of microalgae[14] and distiller's grains.[25] Before applying the Taguchi method to analyze the effects of operating parameters on the HTC process and produced hydrochars, it is important to identify the control parameters and reasonable levels.

Generally, reaction temperature and time are important factors affecting a chemical reaction. For the HTC process of lignocellulosic biomass, temperatures around 200 °C were the most common choice, for example, 200 °C for pine needles, pine cones, and oak leaves;[17] 170−195 °C for wheat straw;[18] 200 °C for pine sawdust;[19] 190−210 °C for distiller's grains;[25] 200 °C for coconut fiber matting and banana pseduostem;[26] and 180 °C for sugar cane bagasse.[27] Reaction times varied from a few minutes to 24 h.

In many HTC processes, acids were added as catalysts, such as citric acid,[14,17,19,28] acrylic acid,[29] and sulfuric acid.[30] Citric acid was chosen because it is the most commonly used acid catalyst for HTC process. The weight percentage of solid feed was another interesting parameter to investigate. It was found that the weight percentage of solid feed is the most important parameter for high carbon recovery rate during hydrochar production from microalgae.[14]

Although no investigation has been reported on the effect of particle size of feedstock on the HTC process, several researches were conducted to study the effect of particle size on the pyrolysis process.[31−33] The particle size can have a significant effect on biochar yield of slow pyrolysis of agricultural residues.[32] Therefore, it is also interesting to study the effect of particle size on the HTC process.

The five control parameters considered in this study are reaction time, catalyst mass, solid mass, reaction temperature, and particle size. Table 2 gives the different levels used for the five control parameters. The experiments have been readily designed to 16 runs by the orthogonal array $L_{16}(4^5)$ as shown in Table 3.

Table 2. Control Factors and Their Levels Used in This Study

factor	description	level 1	level 2	level 3	level 4
A	time (hour)	2	4	8	16
B	catalyst mass (mg)	10	20	40	80
C	solid mass (g)	2.5	5.0	7.5	10.0
D	reaction temperature (°C)	180	190	200	210
E	particle size (μm)	<150	150−300	300−600	>600

RESULTS AND DISCUSSION

Hydrochar Characterization. The *S. horneri* derived hydrochar samples have been studied in detail by various analytical methods.

Composition Analysis. Ultimate analysis (carbon, hydrogen, oxygen, sulfur, and nitrogen contents) and proximate analysis (moisture content, volatile matter, fixed carbon, and ash contents) for *S. Horneri* and its derived hydrochars, along with mass yield and carbon recovery rate are shown in Table 4. The proximate analysis showed that hydrochars had lower moisture content and ash content and higher volatile matter and fixed carbon compared to the raw material. The fixed carbon represents carbon that is not easily biodegraded and has potential for ground burial for carbon credits. Table 4 sample 2 showed that for every 100 tonnes of macroalgae, hydrothermal carbonization at 180 °C yields 74.7 tonnes of hydrochar for ground burial, of which 24.2 tonnes of carbon can be obtained in its stable form.

The moisture content reduced from 12.2% in the raw material to 3.9−10.8% in hydrochars, indicating more hydrophobic

Table 3. $L_{16}(4^5)$ Orthogonal Array of Taguchi Experimental Conditions

row	sample	A	B	C	D	E	time (h)	catalyst mass (mg)	solid mass (g)	reaction temperature (°C)	particle size (μm)
1	1	1	1	1	1	1	2	10	2.5	180	<150
2	5	1	2	2	2	2	2	20	5.0	190	150−300
3	9	1	3	3	3	3	2	40	7.5	200	300−600
4	13	1	4	4	4	4	2	80	10.0	210	>600
5	10	2	1	2	3	4	4	10	5.0	200	>600
6	14	2	2	1	4	3	4	20	2.5	210	300−600
7	2	2	3	4	1	2	4	40	10.0	180	150−300
8	6	2	4	3	2	1	4	80	7.5	190	<150
9	15	3	1	3	4	2	8	10	7.5	210	150−300
10	11	3	2	4	3	1	8	20	10.0	200	<150
11	7	3	3	1	2	4	8	40	2.5	190	>600
12	3	3	4	2	1	3	8	80	5.0	180	300−600
13	8	4	1	4	2	3	16	10	10.0	190	300−600
14	4	4	2	3	1	4	16	20	7.5	180	>600
15	16	4	3	2	4	1	16	40	5.0	210	<150
16	12	4	4	1	3	2	16	80	2.5	200	150−300

Table 4. Ultimate and Proximate Analysis and Product Yields of Raw *S. horneri* and Its Derived Hydrochars

	ultimate analysis %					proximate analysis %[b]					
sample	C	H	N	S	O[a]	MC	VM	FC	Ash	mass yield[c] %	carbon recovery rate[d] %
S. horneri	26.9	4.2	1.7	0.6	56.5	12.2	60.7	17.0	10.1	–	–
1	45.2	5.6	3.8	0.7	42.3	10.8	64.7	22.3	2.3	52.3	87.8
2	50.5	5.5	2.4	0.4	38.4	4.7	68.5	24.2	2.6	39.8	74.7
3	44.2	5.2	1.6	0.4	42.3	5.0	63.8	25.4	5.9	40.3	66.3
4	36.8	5.1	1.4	0.4	48.4	5.5	61.0	26.0	7.5	38.0	52.0
5	43.3	5.0	2.9	0.4	41.9	7.1	63.8	23.1	6.0	45.1	72.6
6	43.6	5.0	2.7	0.4	44.0	4.8	64.9	26.2	4.1	38.8	62.8
7	37.7	4.7	1.3	0.3	49.0	4.4	64.2	24.7	6.6	34.5	48.4
8	47.4	4.8	1.9	0.6	40.7	5.0	66.0	24.6	4.5	38.9	68.5
9	38.1	4.8	2.2	0.3	52.9	6.9	64.3	27.3	1.6	39.1	55.5
10	37.0	4.3	1.5	0.3	54.3	5.6	64.0	28.1	2.4	33.3	45.8
11	43.0	5.0	2.5	0.4	46.8	5.9	64.5	27.4	2.2	38.0	60.9
12	48.5	4.9	2.2	0.3	40.5	4.7	64.9	27.0	3.4	32.7	59.1
13	37.7	5.0	1.7	0.3	54.1	5.7	68.4	24.8	1.2	35.9	50.3
14	45.5	4.9	1.7	0.4	45.9	6.1	67.0	25.4	1.5	35.3	59.7
15	46.8	4.9	2.2	0.4	40.4	5.2	62.6	27.3	4.9	38.5	67.0
16	41.7	4.8	2.5	0.3	44.6	3.9	63.7	26.5	6.0	36.1	55.9

[a]Estimated by difference [O = 100 − (C + H + N + S + Ash)]. [b]MC: moisture content. VM: volatile matter. FC: fixed carbon. [c]Mass yield % = g hydrochar/mass of raw material × 100% [d]Carbon recovery rate = C% in hydrochar/C% in raw material × mass yield%

surface was produced by the HTC process. The ash content was 10.1% in the raw material, which is close to the lower end values of the ash content for macroalgae.[34] The ash content decreased to 1.2−7.5% in its hydrochars. Lower ash content could be due to the removal of the soluble inorganic fraction, such as the alkaline and alkaline earth metals and their salts. A similar result was reported by Murakami et al.,[35] whose ash content of *S. horneri* after boiling in a mixture of seawater and tap water was 1.83%.

After the HTC process, the carbon content increased from 26.9% in the raw material to 36.8−50.5% in the hydrochar samples. The carbon content in hydrochar is strongly dependent on hydrothermal processing conditions and the carbon content in its feedstock. As shown in Figure 1, the carbon content for most biomass in general increases by about 50% after HTC treatment. The results from *S. horneri* showed a similar trend. However, the carbon content in *S. horneri*-derived hydrochars had lower carbon content than most of other reported biomass-derived hydrochars due to lower carbon content in *S. horneri*. The mass yields obtained from the HTC process are in the 33−

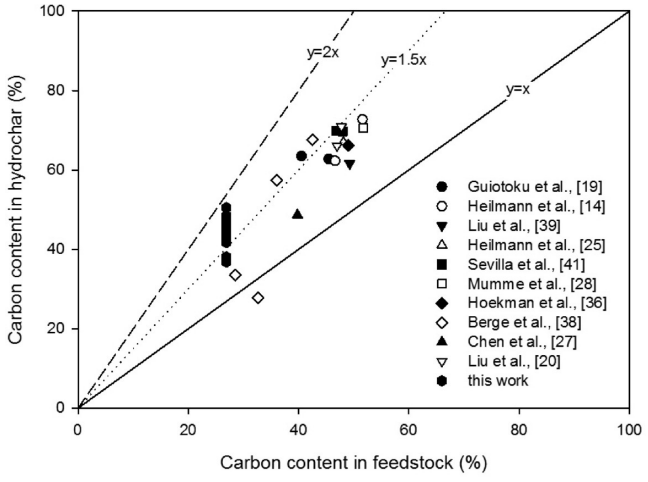

Figure 1. Carbon content in hydrochars vs carbon content in feedstocks. Data was obtained from literature and this work.

52% range (Table 4). On the basis of carbon recovery rates, about 46−88% of carbon content in the raw material was retained in the hydrochar samples. In contrast, the carbon recovery rates were lower for microalgae after the HTC process, in the range of 38−60%,[14] and also for distiller's grains, in the range of 40−58%.[25] For anaerobically digested maize silage, the carbon recovery rates after the HTC process are higher, in the range of 57.6−83.2%.[28]

To evaluate the carbonization process, H/C and O/C atomic ratios of the raw material and its derived hydrochars were plotted in a van Krevelen diagram (Figure 2). The van Krevelen diagram

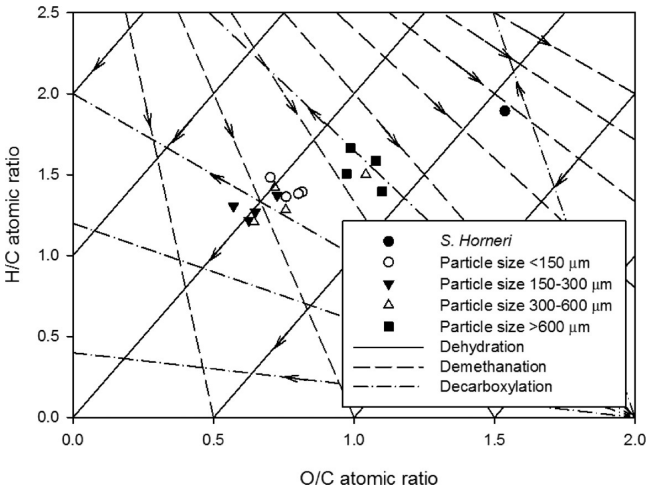

Figure 2. van Krevelen diagram for raw *S. horneri* and its derived hydrochars.

provides information about the reaction pathways during carbonization. The solid line and dash line with arrows in Figure 2 represent the reaction pathway of dehydration and decarboxylation. As shown in Figure 2, the HTC process of *S. horneri* is mainly a dehydration process accompanied with decarboxylation. This HTC pathway is similar to that of other kind of biomass.[28] Therefore, the similarities in the carbonization process and product are due to the similarities in the original lignocellulosic composition of *S. horneri* with other biomass.

Energy Properties of Hydrochars. Heat value is one of the most important characteristics of biomass and their derivatives. It indicates the total amount of energy that is available in a sample. In this study, the higher heating values (HHVs) of the feedstock and hydrochar samples were experimentally determined using a bomb calorimeter. The calculated energy densification ratio is used to evaluate the efficiency of a biomass treatment process. The energy densification ratio is defined as the HHV of a hydrochar sample divided by the HHV of its initial feedstock.[36] The values for HHV and the energy densification ratio for the feedstock and all hydrochar samples are provided in Table 5.

The feedstock, *S. horneri*, had a HHV of 17.4 MJ kg^{-1}, while the HHVs of its derived hydrochars were in the range of 19.0−25.1 MJ kg^{-1}. After hydrothermal treatment, the biomass has been upgraded to have a similar HHV to subbituminous coal.[37] The HHVs of hydrochars are strongly depended on their initial feedstock composition. Berge et al.[38] reported the hydrochars derived from food waste, paper waste, mixed municipal waste stream, and anaerobic digestion waste have HHVs of 29.1, 23.9, 20.0, and 13.7 MJ kg^{-1}, respectively. Under different reaction conditions, the HHVs of the hydrochars produced from a wood mixture range from 22.5 to 29.5 MJ kg^{-1}.[36] When a similar

Table 5. Energy and Physical and Chemical Properties of Raw *S. horneri* and Its Derived Hydrochars

sample	HHV[a] MJ kg^{-1}	energy densification ratio[b]	pH	surface area m^2 g^{-1}
S. horneri	17.4	–	6.2	–
1	20.8	1.20	5.1	0.6
2	22.7	1.31	5.0	16.3
3	22.9	1.32	4.1	27.4
4	21.3	1.23	5.5	21.9
5	21.2	1.22	4.5	1.6
6	20.2	1.16	5.0	20.0
7	21.6	1.24	5.1	27.7
8	23.9	1.38	5.7	21.0
9	21.0	1.21	4.7	1.8
10	21.0	1.21	4.6	31.8
11	19.0	1.10	6.3	13.2
12	24.4	1.40	5.9	21.0
13	22.4	1.29	4.6	22.6
14	22.9	1.32	5.0	24.8
15	25.1	1.44	6.0	16.6
16	25.1	1.45	6.4	15.5

[a]Higher heating value based on dry weight. [b]Energy densification ratio = $HHV_{sample}/HHV_{feedstock}$.

hydrothermal process was applied on microalgae, it can produce a hydrochar with a high HHV of 31 MJ kg^{-1}.[14] The maize silage-derived hydrochars are found to have high HHVs of 25−36 MJ kg^{-1}, estimated by Mott and Spooner's correlation based on elemental composition.[28]Therefore, hydrochars from *S. horneri* had HHV values closer to wood and paper waste due to their similar lignocellulosic composition in the source material.

To study the efficiency of the hydrothermal treatment of *S. Horneri*, energy densification ratios were determined. The energy densification ratios were found to be in the range of 1.10−1.45. They were close to the values previously reported in literature for wheat straw[18] and wood waste.[36] Hydrothermal treatment on wheat straw at 180 °C increased the HHV from 15.2 to 17.3−18.6 MJ kg^{-1}, which equals to the energy densification ratios of 1.14−1.22.[18] Energy density increases of 11−45% are reported with for a hydrothermal treatment of wood mixture at 215−295 °C.[36] Higher energy densification ratios of 1.5−2.2 are achieved by applying a hydrothermal treatment to municipal waste streams.[38] Therefore, hydrochars show a high potential for use as a solid fuel and justify further exploration in this area.

Chemical Properties of Hydrochars. The pH values of hydrochars in water, ranging from 4.1 to 6.4, are in general lower than the ones of raw *S. Horneri* powers (Table 5). The lower pH could be due to the existence of acid functional groups such as carboxyl, lactone, phenol, etc. It is reported that the majority of hydrochars are more acidic than biochars produced by pyrolysis, which are often alkaline.[5] For example, the hydrochars produced from pinewood at 300 °C have pH values of 3.80, while the pH value of the biochar obtained at 700 °C by pyrolysis is 6.60.[39] It was explained that more carboxylic groups were in hydrochar than in biochar. Similarly, the hydrochars produced from beet root chips and bark chips have pH values of 4.8 and 5.2 in aqueous solutions, while biochars produced by pyrolysis from the same materials have pH values of 8.4−10.3.[40]

The FT-IR spectra of raw *S. horneri* and hydrochars were used to examine the surface functional groups. The FT-IR spectra of feedstock and two selected hydrochar samples are illustrated in Figure 3. Hydrochar sample 16 had the highest pH value of 6.4,

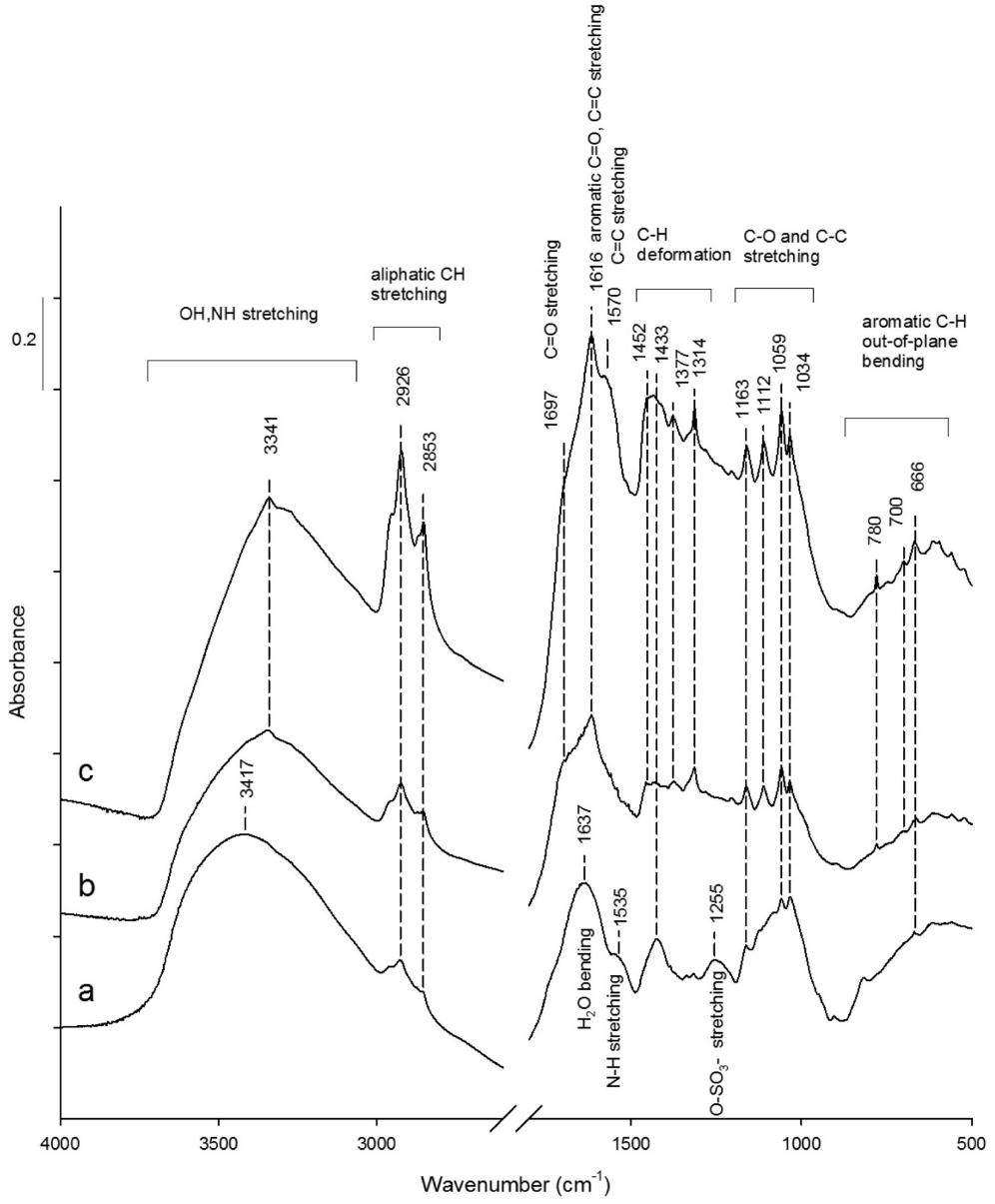

Figure 3. FT-IR spectra of (a) raw material, (b) hydrochar sample 3 (t = 2 h, catalyst mass = 40 mg, solid mass = 7.5 g, T = 200 °C, and particle size = 300−600 μm), and (c) hydrochar sample 16 (t = 16 h, catalyst mass = 80 mg, solid mass = 2.5 g, T = 200 °C, and particle size = 150−300 μm).

while hydrochar sample 3 had the lowest pH value of 4.1. The various IR absorption bands were assigned based on the literature.[41,42] Both feedstock and their hydrochar products had a broad absorption band at 3000−3600 cm^{-1}, attributed to OH stretching vibration in the hydroxyl or carboxyl groups.[41] However, the center of the band was shifted from 3417 cm^{-1} for the raw material to 3341 cm^{-1} for the hydrochar samples, indicating intermolecular hydrogen bond formation after hydrothermal carbonization. The hydrochars had stronger absorption bands at 3000−2800 cm^{-1}, which attributes to stretching vibrations of aliphatic C−H. It indicates that aliphatic hydrocarbon was formed during the hydrothermal carbonization process. The similar phenomenon was also reported by Steinbeiss et al.[43] For acid group (C═OOH), there were strong stretching peaks in the following region: 1700−1725 cm^{-1}(C═O), 2500−3300 (O−H) broad peak, and 1210−1320 (C−O). In all cases, conjugation in the (C═O) double bond have shifted the wavenumber lower. The results here indicate the acidity may be due more to phenolic groups, as aromatic stretch regions (1600 cm^{-1}, multiple bands) and increased OH stretching (300−3700 cm^{-1}), which show strong absorbance bands. The bands appearing in hydrochar samples at 600−800 cm^{-1} were assigned to aromatic C−H out-of-plane bending vibrations.[44]

Morphology and Structural Properties of Hydrochars. The morphology of *S. horneri* and its derived hydrochars has been studied by scanning electron microscopy (SEM). SEM images of the raw materials and selected hydrochar samples are shown in Figure 4. The original morphology of the particles is mainly preserved after the HTC process, while the surface became rougher due to the treatment. Microspheres with diameters of several micrometers were observed in some of the hydrochar samples. Similar microspheres are also observed on the hydrochars derived from various types of feedstock.[17,28,41,44] These microspheres are thought to be formed during the HTC of cellulose[45] and soluble carbohydrate components.[17]

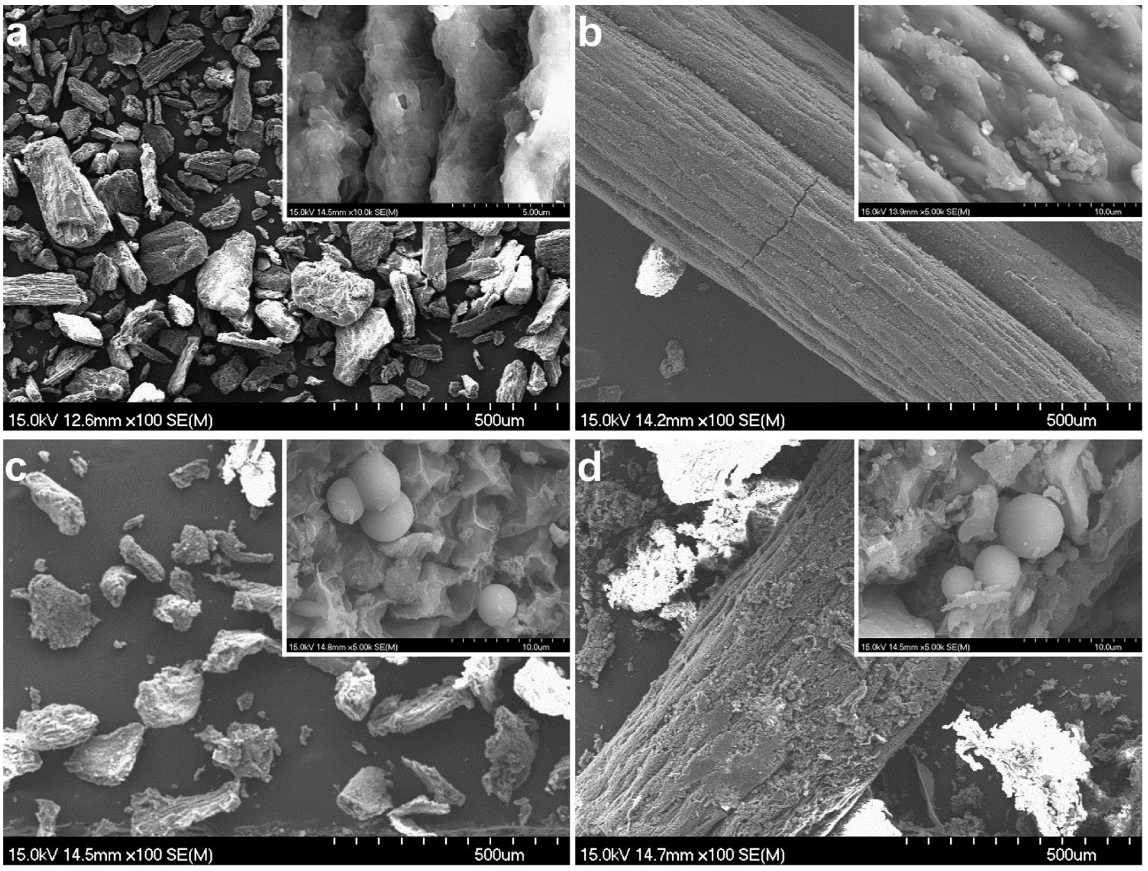

Figure 4. SEM images of selected raw *S. horneri*, (a) <150 μm and (b) >600 μm, and selected derived hydrochar, (c) sample 6 and (d) sample 7. Magnification for main images and insets are 100 and 5000, respectively.

The porous structure of hydrochars was characterized by nitrogen sorption measurements. The N_2 sorption isotherms of all samples shared the same shape (Figure 5). They had Type H3 hysteresis loops above $p/p0$ = 0.45 without any limiting adsorption at high relative pressure. It indicated slit-shaped pores in aggregates of plate-like particles. Dried *S. horneri* powder showed no detectable porosity.

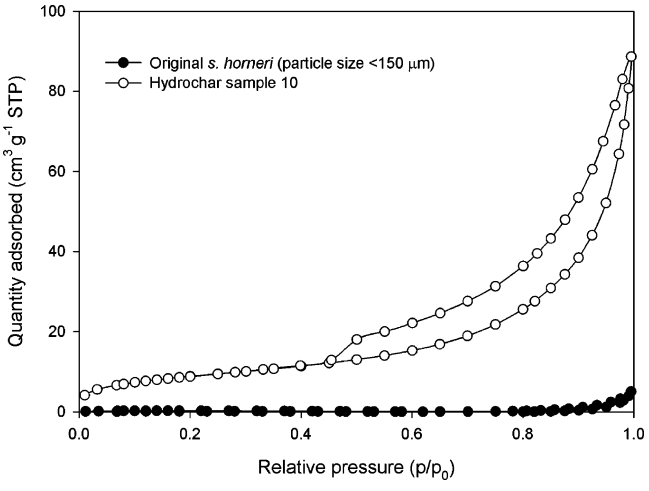

Figure 5. N_2 sorption isotherms for raw *S. horneri* (particle size < 150 μm) and hydrochar sample 10 (reaction conditions: t = 4 h, catalyst mass = 10 mg, solid mass = 5.0 g, T = 200 °C, and particle size > 600 μm).

As shown in Table 5, the BET surface area was generally low for hydrochars produced at all conditions, ranging from 0.6 to 31.8 $m^2\ g^{-1}$. It is consistent with previous studies on biomass-derived hydrochars. Titirici et al. reported BET surface areas for hydrochars obtained from pine needle, oak leaf, and pine cone of 12, 15.5, and 34 $m^2\ g^{-1}$, respectively.[17] Liu et al. found a BET surface area of 21 $m^2\ g^{-1}$ for pinewood-derived hydrochars.[39] Digestate of maize silage can achieve a 12 $m^2\ g^{-1}$ BET surface area by hydrothermal carbonization.[28] Hydrochars derived from coconut fiber matting and banana pseudostem had surface areas of 48 and 8 $m^2\ g^{-1}$, respectively.[26] Limited porosity and low surface area is, however, one limitation for hydrochars, and potential use of hydrochars for its surface activity, such as adsorbents and catalysts, is limited under the experimental conditions. For catalytic or energetic applications, it is necessary to improve the hydrochar's porosity and surface area by combination of thermal and chemical activation. For example, H_3PO_4 activation can obtain activated carbon with a BET surface area over 2500 $m^2\ g^{-1}$ from hydrochars.[26] Chemical activation with KOH at 700 °C can produce activated carbon with high surface areas up to 2700 $m^2\ g^{-1}$.[46]

Effects of Control Factors. The effects of control factors on the carbon recovery rate (%), HHV, hydrochar pH, and BET surface area were studied by multiple linear regression and graphical methods. These four important outputs were selected to represent the level of carbonization, energy, and chemical and physical properties of hydrochars, respectively. The multiple linear regression equations developed from the Taguchi method are as follows

dx.doi.org/10.1021/sc400118f | ACS Sustainable Chem. Eng. 2013, 1, 1092−1101

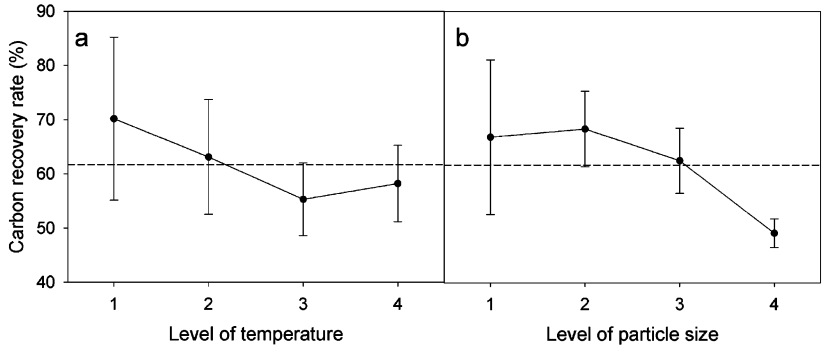

Figure 6. Dependence of carbon recovery rate on the process parameters using Taguchi method.

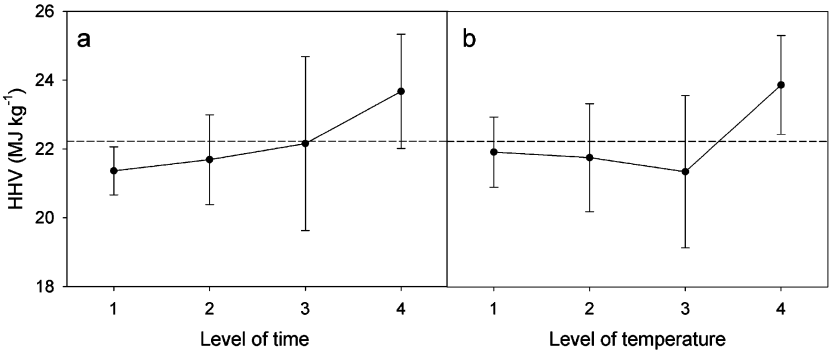

Figure 7. Dependence of HHV of hydrochars on the process parameters using Taguchi method.

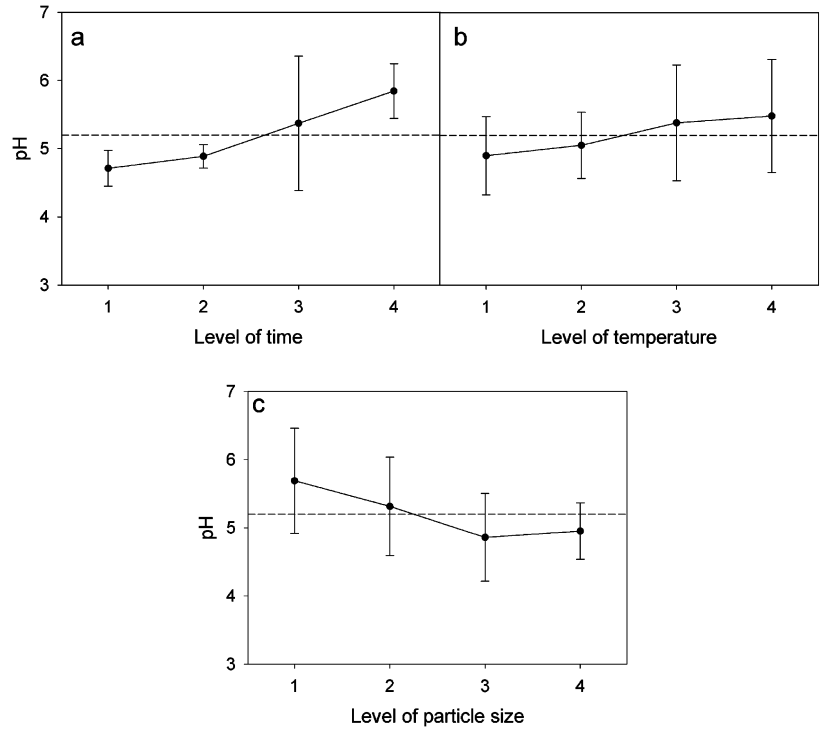

Figure 8. Dependence of the pH value of hydrochars in water on the process parameters using Taguchi method.

$$\text{Carbon recovery rates} = 1.57 - 4.37 \times 10^{-3}T - 2.41 \times 10^{-4}D \quad (1)$$

$$\text{HHV} = 19.54 + 1.89 \times 10^{-1}t \quad (2)$$

$$\text{pH in water} = 8.85 \times 10^{-1} + 8.13 \times 10^{-2}t + 2.08 \times 10^{-2}T - 8.29 \times 10^{-4}D \quad (3)$$

$$\text{BET surface area} = 10.43 + 1.74 \times 10^{-2}D \quad (4)$$

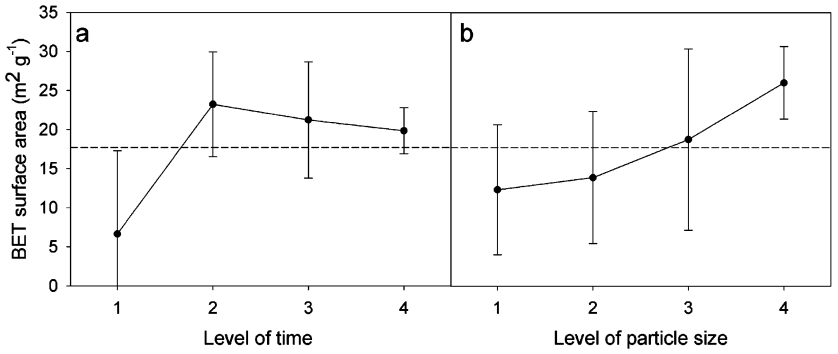

Figure 9. Dependence of BET surface area of hydrochars on the process parameters using Taguchi method.

where t is the reaction time in hours, T is the reaction temperature in °C, and D is the particle size in μm. The control factor with a p-value less than 0.05 was considered to be significant. Only significant control factors are listed in the linear regression equations.

For carbon recovery rate, reaction temperature and particle size are the two significant control factors. Higher reaction temperature led to lower carbon recovery rate, as shown in Figure 6, which was due to more decarboxylation at higher temperature. Figure 6 shows that higher carbon recovery rate can be achieved with the raw materials with smaller particle size. The hydrochars derived from the raw materials with smaller particle size also had both lower O/C and H/C atomic ratio (Figure 2). Therefore, it can be concluded that smaller particle size lead to more complete dehydration.

For HHV, reaction time is the only significant control factor with a p-value of 0.031. As shown in Figure 7a, the HHVs increased with increasing reaction time. Similar findings were reported by Hoekman et al.[36] for hydrothermal treatment of wood mixture. The HHVs of produced hydrochars had HHVs of 25.1, 26.0, and 29.2 MJ kg^{-1} for 5, 10, and 60 min reaction time at 255 °C, respectively. Higher HHVs of hydrochars could be caused by more complete carbonization[28] due to rearrangement and change in conformation of molecules with time. It was also found that reaction temperature had no effect on the HHVs of produced hydrochars in the temperature range of 180−200 °C, while the average HHVs increased by 12% when temperature increased from 200 to 210 °C (Figure 7b). Hoekman et al. found that HHV of hydrochar increases with increasing reaction temperature in the temperature range of 215 to 255 °C and reaches plateau when temperature exceeded 255 °C. Therefore, it could be concluded that reaction temperature only has significant effect on HHVs of produced hydrochar at higher a temperature range, where degradation of cellulose and lignin becomes significant.

The reaction time, reaction temperature, and particle size are all significant control factors for hydrochar pH values in water. Among them, reaction time was the most important factor with a p-value less than 0.001. Longer reaction time and higher reaction temperature led to high pH value (Figure 8a,b), which was due to more complete carbonization. Larger particle size had a hindering effect on carbonization process. Therefore, it was found that larger particle size led to lower pH of hydrochars in aqueous solution (Figure 8c).

For BET surface area, particle size was the only significant control factor with a p-value of 0.025. The average BET surface area for the starting material with a particle size less than 150 μm was 12.3 m^2 g^{-1}. With increasing particle size, the average BET surface area increased to 13.9, 18.8, and 26.0 m^2 g^{-1} for the starting materials with a particle size of 150−300 μm, 300−600 μm, and greater than 600 μm, respectively (Figure 9b). As mentioned above, larger particle size led to less carbonization. Liu et al.[39] explained a similar finding by the cracking and blocking of pore structure. As the carbonization process goes on, the softening and melting of biomass constituents could partially block the pore structure, which could lead to lower surface area. It is also interesting to note that the average BET surface area for a 2 h reaction time was much lower than the ones for the other three levels of reaction time (Figure 9a). This indicates that in order to reach a reasonable BET surface area a reaction time longer than 4 h was necessary.

CONCLUSIONS

The hydrothermal carbonization process was applied to *S. horneri* to produce hydrochars at mild conditions of 180−210 °C for 2−16 h with citric acid as catalyst. The carbonization process increased the carbon content by up to 50%. The highest HHV achieved after HTC process was 25.1 MJ kg^{-1}, with very low ash content and relatively high yield. Therefore, there is potential for hydrochars from *S. horneri* to be used as a solid fuel. Among the five control factors tested, it was found that reaction temperature, reaction time, and the particle size were the most important parameters for controlling the HTC process.

AUTHOR INFORMATION

Corresponding Author

*E-mail: augustine.quek@nottingham.edu.cn (A.Q.); jiawei.wang@nottingham.edu.cn (J.W.). Tel: +86 574 8818 9130. Fax: +86 574 8818 0175.

Author Contributions

The manuscript was written through contributions of all authors. All authors have given approval to the final version of the manuscript.

Notes

The authors declare no competing financial interest.

ACKNOWLEDGMENTS

The authors thank Mr. Tiegan Wang of Zhejiang Mariculture Research Institute and Mr. Qinghai Sun of Wenzhou Seatiger Seaweed Cultivation Co., Ltd. for providing the raw materials. J.W. thanks the financial support from the Faculty of Science and Engineering of University of Nottingham Ningbo China and Ningbo Science and Technology Bureau (2012B82011). G.Z. thanks the financial support from the Natural Science Foundation of Zhejiang Province (LY12D06004) and the Public

Welfare project of the Science and Technology Committee of Zhejiang Province (2011C23071).

REFERENCES

(1) Saidur, R.; Abdelaziz, E. A.; Demirbas, A.; Hossain, M. S.; Mekhilef, S. A review on biomass as a fuel for boilers. *Renew. Sust. Energy Rev.* **2011**, *15* (5), 2262−2289.

(2) McKendry, P. Energy production from biomass (part 2): Conversion technologies. *Bioresour. Technol.* **2002**, *83* (1), 47−54.

(3) Titirici, M.-M.; Antonietti, M. Chemistry and materials options of sustainable carbon 22 materials made by hydrothermal carbonization. *Chem. Soc. Rev.* **2010**, *39* (1), 103−116.

(4) Hu, B.; Wang, K.; Wu, L.; Yu, S.-H.; Antonietti, M.; Titirici, M.-M. Engineering carbon materials from the hydrothermal carbonization process of biomass. *Adv. Mater.* **2010**, *22* (7), 813−828.

(5) Libra, J. A.; Ro, K. S.; Kammann, C.; Funke, A.; Berge, N. D.; Neubauer, Y.; Titirici, M.-M.; Fühner, C.; Bens, O.; Kern, J.; Emmerich, K.-H. Hydrothermal carbonization of biomass residuals: A comparative review of the chemistry, processes and applications of wet and dry pyrolysis. *Biofuels* **2011**, *2* (1), 89−124.

(6) Titirici, M.-M.; White, R. J.; Falco, C.; Sevilla, M. Black perspectives for a green future: Hydrothermal carbons for environment protection and energy storage. *Energy Environ. Sci.* **2012**, *5* (5), 6796−6822.

(7) Aresta, M.; Dibenedetto, A.; Barberio, G. Utilization of macro-algae for enhanced CO_2 fixation and biofuels production: Development of a computing software for an LCA study. *Fuel Process. Technol.* **2005**, *86* (14−15), 1679−1693.

(8) Bruhn, A.; Dahl, J.; Nielsen, H. B.; Nikolaisen, L.; Rasmussen, M. B.; Markager, S.; Olesen, B.; Arias, C.; Jensen, P. D. Bioenergy potential of *Ulva lactuca*: Biomass yield, methane production and combustion. *Bioresour. Technol.* **2011**, *102* (3), 2595−2604.

(9) Kim, N.-J.; Li, H.; Jung, K.; Chang, H. N.; Lee, P. C. Ethanol production from marine algal hydrolysates using *Escherichia coli* KO11. *Bioresour. Technol.* **2011**, *102* (16), 7466−7469.

(10) Harun, R.; Danquah, M. K.; Forde, G. M. Microalgal biomass as a fermentation feedstock for bioethanol production. *J. Chem. Technol. Biotechnol.* **2010**, *85* (2), 199−203.

(11) Takeda, H.; Yoneyama, F.; Kawai, S.; Hashimoto, W.; Murata, K. Bioethanol production from marine biomass alginate by metabolically engineered bacteria. *Energy Environ. Sci.* **2011**, *4* (7), 2575−2581.

(12) Kucukvar, M.; Tatari, O. A comprehensive life cycle analysis of cofiring algae in a coal power plant as a solution for achieving sustainable energy. *Energy* **2011**, *36* (11), 6352−6357.

(13) Agrawal, A.; Chakraborty, S. A kinetic study of pyrolysis and combustion of microalgae *Chlorella vulgaris* using thermogravimetric analysis. *Bioresour. Technol.* **2013**, *128*, 72−80.

(14) Heilmann, S. M.; Davis, H. T.; Jader, L. R.; Lefebvre, P. A.; Sadowsky, M. J.; Schendel, F. J.; von Keitz, M. G.; Valentas, K. J. Hydrothermal carbonization of microalgae. *Biomass Bioenergy* **2010**, *34* (6), 875−882.

(15) Falco, C.; Sevilla, M.; White, R. J.; Rothe, R.; Titirici, M.-M. Renewable nitrogen-doped hydrothermal carbons derived from micro-algae. *ChemSusChem* **2012**, *5* (9), 1834−1840.

(16) Gao, K.; McKinley, K. R. Use of macroalgae for marine biomass production and CO_2 remediation: A review. *J. Appl. Phycol.* **1994**, *6* (1), 45−60.

(17) Titirici, M. M.; Thomas, A.; Yu, S.-H.; Mueller, J.-O.; Antonietti, M. A direct synthesis of mesoporous carbons with bicontinuous pore morphology from crude plant material by hydrothermal carbonization. *Chem. Mater.* **2007**, *19* (17), 4205−4212.

(18) Thomsen, M. H.; Thygesen, A.; Thomsen, A. B. Hydrothermal treatment of wheat straw at pilot plant scale using a three-step reactor system aiming at high hemicellulose recovery, high cellulose digestibility and low lignin hydrolysis. *Bioresour. Technol.* **2008**, *99* (10), 4221−4228.

(19) Guiotoku, M.; Rambo, C. R.; Hansel, F. A.; Magalhães, W. L. E.; Hotza, D. Microwave-assisted hydrothermal carbonization of lignocellulosic materials. *Mater. Lett.* **2009**, *63* (30), 2707−2709.

(20) Liu, Z.; Quek, A.; Kent Hoekman, S.; Balasubramanian, R. Production of solid biochar fuel from waste biomass by hydrothermal carbonization. *Fuel* **2013**, *103*, 943−949.

(21) Choi, H.; Lee, K.; Yoo, H.; Kang, P.; Kim, Y.; Nam, K. Physiological differences in the growth of Sargassum horneri between the germling and adult stages. *J. Appl. Phycol.* **2008**, *20* (5), 729−735.

(22) Pang, S.; Liu, F.; Shan, T.; Gao, S.; Zhang, Z. Cultivation of the brown alga *Sargassum horneri*: Sexual reproduction and seedling production in tank culture under reduced solar irradiance in ambient temperature. *J. Appl. Phycol.* **2009**, *21* (4), 413−422.

(23) Munir, S.; Daood, S. S.; Nimmo, W.; Cunliffe, A. M.; Gibbs, B. M. Thermal analysis and devolatilization kinetics of cotton stalk, sugar cane bagasse and shea meal under nitrogen and air atmospheres. *Bioresour. Technol.* **2009**, *100* (3), 1413−1418.

(24) Carrier, M.; Hardie, A. G.; Uras, Ü.; Görgens, J.; Knoetze, J. J. Production of char from vacuum pyrolysis of South African sugar cane bagasse and its characterization as activated carbon and biochar. *Anal. Appl. Pyrol.* **2012**, *96*, 24−32.

(25) Heilmann, S. M.; Jader, L. R.; Sadowsky, M. J.; Schendel, F. J.; von Keitz, M. G.; Valentas, K. J. Hydrothermal carbonization of distiller's grains. *Biomass Bioenergy* **2011**, *35* (7), 2526−2533.

(26) Romero-Anaya, A. J.; Lillo-Ródenas, M. A.; Salinas-Martínez de Lecea, C.; Linares-Solano, A. Hydrothermal and conventional H_3PO_4 activation of two natural bio-fibers. *Carbon* **2012**, *50* (9), 3158−3169.

(27) Chen, W.-H.; Ye, S.-C.; Sheen, H.-K. Hydrothermal carbonization of sugarcane bagasse via wet torrefaction in association with microwave heating. *Bioresour. Technol.* **2012**, *118* (0), 195−203.

(28) Mumme, J.; Eckervogt, L.; Pielert, J.; Diakite, M.; Rupp, F.; Kern, J. Hydrothermal carbonization of anaerobically digested maize silage. *Bioresour. Technol.* **2011**, *102* (19), 9255−9260.

(29) Demir-Cakan, R.; Baccile, N.; Antonietti, M.; Titirici, M.-M. Carboxylate-rrich carbonaceous materials via one-step hydrothermal carbonization of glucose in the presence of acrylic acid. *Chem. Mater.* **2009**, *21* (3), 484−490.

(30) Liang, X.; Yang, J. Synthesis of a novel carbon based strong acid catalyst through hydrothermal carbonization. *Catal. Lett.* **2009**, *132* (3−4), 460−463.

(31) Şensöz, S.; Angın, D.; Yorgun, S. Influence of particle size on the pyrolysis of rapeseed (*Brassica napus* L.): Fuel properties of bio-oil. *Biomass Bioenergy* **2000**, *19* (4), 271−279.

(32) Demirbas, A. Effects of temperature and particle size on bio-char yield from pyrolysis of agricultural residues. *J. Anal. Appl. Pyrol.* **2004**, *72* (2), 243−248.

(33) Encinar, J. M.; Beltrán, F. J.; Bernalte, A.; Ramiro, A.; González, J. F. Pyrolysis of two agricultural residues: Olive and grape bagasse. Influence of particle size and temperature. *Biomass Bioenergy* **1996**, *11* (5), 397−409.

(34) Marinho-Soriano, E.; Fonseca, P. C.; Carneiro, M. A. A.; Moreira, W. S. C. Seasonal variation in the chemical composition of two tropical seaweeds. *Bioresour. Technol.* **2006**, *97*, 2402−2406.

(35) Murakami, K.; Yamaguchi, Y.; Noda, K.; Fujii, T.; Shinohara, N.; Ushirokawa, T.; Sugawa-Katayama, Y.; Katayama, M. Seasonal variation in the chemical composition of a marine brown alga, *Sargassum horneri* (Turner) C. Agardh. *J. Food Comp. Anal.* **2011**, *24*, 231−236.

(36) Hoekman, S. K.; Broch, A.; Robbins, C. Hydrothermal carbonization (HTC) of lignocellulosic biomass. *Energy Fuels* **2011**, *25* (4), 1802−1810.

(37) Smoot, L. D.; Smith, P. J. *Coal Combustion and Gasification*; Springer: New York, 1985.

(38) Berge, N. D.; Ro, K. S.; Mao, J.; Flora, J. R. V.; Chappell, M. A.; Bae, S. Hydrothermal carbonization of municipal waste streams. *Environ. Sci. Technol.* **2011**, *45* (13), 5696−5703.

(39) Liu, Z.; Zhang, F.-S.; Wu, J. Characterization and application of chars produced from pinewood pyrolysis and hydrothermal treatment. *Fuel* **2010**, *89* (2), 510−514.

(40) Kammann, C.; Ratering, S.; Eckhard, C.; Müller, C. Biochar and hydrochar effects on greenhouse gas (carbon dioxide, nitrous oxide, and methane) fluxes from soils. *J. Environ. Qual.* **2012**, *41* (4), 1203−1209.

(41) Sevilla, M.; Maciá-Agulló, J. A.; Fuertes, A. B. Hydrothermal carbonization of biomass as a route for the sequestration of CO_2: Chemical and structural properties of the carbonized products. *Biomass Bioenergy* **2011**, *35* (7), 3152−3159.
(42) Kumar, S.; Loganathan, V. A; Gupta, R. B.; Barnett, M. O. An assessment of U(VI) removal from groundwater using biochar produced from hydrothermal carbonization. *J. Environ. Manag.* **2011**, *92*, 2504−2512.
(43) Steinbeiss, S.; Gleixner, G.; Antonietti, M. Effect of biochar amendment on soil carbon balance and soil microbial activity. *Soil Biol. Biochem.* **2009**, *41* (6), 1301−1310.
(44) Wang, L.; Guo, Y.; Zhu, Y.; Li, Y.; Qu, Y.; Rong, C.; Ma, X.; Wang, Z. A new route for preparation of hydrochars from rice husk. *Bioresour. Technol.* **2010**, *101* (24), 9807−9810.
(45) Sevilla, M.; Fuertes, A. B. The production of carbon materials by hydrothermal carbonization of cellulose. *Carbon* **2009**, *47* (9), 2281−2289.
(46) Sevilla, M.; Fuertes, A. B.; Mokaya, R. High density hydrogen storage in superactivated carbons from hydrothermally carbonized renewable organic materials. *Energy Environ. Sci.* **2011**, *4* (4), 1400−1410.